

Interparticle correlations in the production of J/ψ pairs in proton-proton collisions

S. P. Baranov*

P.N. Lebedev Institute of Physics, Lenin Avenue 53, 119991 Moscow, Russia

A. M. Snigirev† and N. P. Zotov‡

Skobeltsyn Institute of Nuclear Physics, Lomonosov Moscow State University, 119991 Moscow, Russia

A. Szczurek§

*Institute of Nuclear Physics PAN, PL-31-342 Cracow, Poland and
University of Rzeszów, PL-35-959 Rzeszów, Poland*

W. Schäfer¶

*Institute of Nuclear Physics PAN, PL-31-342 Cracow, Poland
(Dated: August 30, 2021)*

We focus on the problem of disentangling the single (SPS) and double (DPS) parton scattering modes in the production of J/ψ pairs at the LHC conditions. Our analysis is based on comparing the shapes of the differential cross sections and on studying their behavior under imposing kinematical cuts. On the SPS side, we consider the leading-order $\mathcal{O}(\alpha_s^4)$ contribution with radiative corrections (taken into account in the framework of the k_t -factorization approach) and the subleading $\mathcal{O}(\alpha_s^6)$ contribution from pseudo-diffractive gluon-gluon scattering represented by one gluon exchange and two gluon exchange mechanisms. We come to the conclusion that disentangling the SPS and DPS modes is rather difficult on the basis of azimuthal correlations, while the rapidity difference looks more promising, provided the acceptance of the experimental detectors has enough rapidity coverage.

PACS numbers: 12.38.Bx, 13.85.Ni, 14.40.Pq

I. INTRODUCTION

Since it was first observed, charmonium production in hadronic collisions has been a subject of considerable theoretical interest. Production rates and their dependence on the different kinematic variables provide important tests for comparing theoretical models.

In the last years, the production of J/ψ pairs has attracted a significant renewal attention in the context of searches for double parton scattering processes [1]. A number of discussions has been stimulated by the recent measurement [2] of the double J/ψ production cross section at the LHCb experiment at CERN. Theoretical estimates based on both collinear [3–5] and k_t -factorization [6] approaches show that the single (SPS) and double (DPS) parton scattering contributions are comparable in size and, taken together, can perfectly describe the measured cross section.

To disentangle the SPS and DPS mechanisms one needs to clearly understand the production kinematics. Naive expectations that the SPS mechanism should result in the back-to-back event configuration received no support from the later calculations. Including the initial state radiation effects (either in the form of k_t -dependent

gluon distributions [7] or by means of simulating the parton showers in a phenomenological way [5]) washes out the original azimuthal correlations, thus making the SPS and DPS samples very similar to each other. One cannot exclude, however, that the situation may change under imposing certain cuts on the J/ψ transverse momenta. On the other hand, it has been suggested [5, 8] that the DPS production is characterized by a much larger rapidity difference between the two J/ψ mesons. The dominance of the DPS contribution over SPS at large rapidity difference was discussed recently also for $pp \rightarrow c\bar{c}c\bar{c}X$ reaction [9, 10]. The goal of the present study is to carefully examine the J/ψ pair production properties in the different kinematical domains paying attention to the different contributing processes. On the SPS side, we consider the leading-order $\mathcal{O}(\alpha_s^4)$ subprocess (with radiative corrections taken into account in the framework of the k_t -factorization approach) and the subleading $\mathcal{O}(\alpha_s^6)$ contribution from pseudo-diffractive gluon-gluon scattering represented by one-gluon exchange and two-gluon exchange mechanisms; the latter mechanisms yet have never been discussed in the context of searches for DPS. On the DPS side, we consider the prompt production of J/ψ pairs including the direct $g + g \rightarrow J/\psi + g$ contribution and radiative χ_c decays.

*Electronic address: baranov@sci.lebedev.ru

†Electronic address: snigirev@lav01.sinp.msu.ru

‡Electronic address: zotov@theory.sinp.msu.ru

§Electronic address: antoni.szczurek@ifj.edu.pl

¶Electronic address: wolfgang.schafer@ifj.edu.pl

II. THEORETICAL FRAMEWORK

A. SPS contributions

At the leading order, $\mathcal{O}(\alpha_s^4)$, the SPS subprocess $g + g \rightarrow J/\psi + J/\psi$ is represented by a set of 31 "box" diagrams, with some examples displayed in Fig. 1. Our approach is based on perturbative QCD, nonrelativistic bound state formalism [11–13], and the k_t -factorization ansatz [14–16] in the parton model. The advantage of using the k_t -factorization approach comes from the ease of including the initial state radiation corrections that are efficiently taken into account in the form of the evolution of gluon densities. The calculation of this subprocess is identical to that described in Ref. [7].

As usual, the production amplitudes contain spin and color projection operators that guarantee the proper quantum numbers of the final state mesons. Then, the J/ψ formation probability is determined by the radial wave function at the origin of coordinate space $|\mathcal{R}(0)|^2$; the latter is known from the J/ψ leptonic decay width [17]. Only the color singlet channels are taken into consideration in the present study since this approach was found to be fully sufficient [18] to describe all of the known LHC data on J/ψ production.

The evaluation of Feynman diagrams is straightforward and follows the standard QCD rules, with one reservation: in accordance with the k_t -factorization prescription [14], the initial gluon spin density matrix is taken in the form $\overline{\epsilon_g^\mu \epsilon_g^{*\nu}} = k_T^\mu k_T^\nu / |k_T|^2$, where k_T is the component of the gluon momentum perpendicular to the beam axis. In the collinear limit, when $k_T \rightarrow 0$, this expression converges to the ordinary $\overline{\epsilon_g^\mu \epsilon_g^{*\nu}} = -g^{\mu\nu}/2$, while in the case of off-shell gluons it contains an admixture of longitudinal polarization. All algebraic manipulations with Feynman diagrams have been done using the computer system FORM [19].

We have carefully checked that our present results are consistent with earlier calculations known in the literature. The model based on the diagrams of Fig. 1 was first formulated in Refs. [20, 21]. Later on, it was extended to considering the polarization effects [22, 23] and to including the color-octet contributions, see [23, 24] and references therein. As far as the color-singlet contribution is concerned, all these papers are fully identical to each other; the calculations are made in the collinear scheme and restricted to the $\mathcal{O}(\alpha_s^4)$ order. Using the k_t -factorization approach we go beyond these approximations by including the initial state radiation corrections. We have checked that in the collinear limit we perfectly reproduce the results of Refs. [20–24].

The full FORTRAN code for the matrix element is available from the authors on request. This process is also available in the hadron level Monte Carlo generator CASCADE [25]. Numerical results shown in the next section have been obtained using the A0 gluon distribution from [26].

In addition to the above, we also consider the pseudo-diffractive gluon-gluon scattering subprocesses represented by the diagrams of Fig. 2. Despite the latter are of formally higher order in α_s , they contribute to the events with large rapidity difference between the two J/ψ mesons and in that region can take over the leading-order 'box' subprocess. Our processes differ from the true diffraction in the sense that there occurs color exchange, and so, the rapidity interval between the two J/ψ 's may be filled up with lighter hadrons (thus showing no gap in the overall hadron density). Among the variety of higher-order contributions, the pseudo-diffractive subprocesses mentioned here are of our special interest as they potentially can mimic the DPS mechanism having very similar kinematics.

The evaluation of the one-gluon exchange diagrams $g(k_1) + g(k_2) \rightarrow J/\psi(p_1) + J/\psi(p_2) + g(k_3) + g(k_4)$ is straightforward, but the number of diagrams is rather large. There are six possible gluon permutations in the upper quark loop and six permutations in the lower loop. Besides that, we have to consider interchanges between the two initial or two final gluons: $g(k_1) \leftrightarrow g(k_2)$, $g(k_3) \leftrightarrow g(k_4)$, thus ending up with 144 possible combinations. Note that the matrix element is free from infrared singularities. This is due to the specific property of the quark loop amplitude which vanishes when any of the three attached gluons becomes soft. These calculations have also been performed in the k_t -factorization approach as described above.

The two gluon exchange mechanism has been previously considered in Ref. [27], where it was reduced to the production of J/ψ pairs in photon-photon collisions [28] by recalculating the appropriate color factor. We basically follow the same way in our present analysis, but use an updated gluon density [29].

Let us concentrate on the elementary $g+g \rightarrow J/\psi+J/\psi$ subprocess first. Only 16 of the different possible Feynman diagrams survive in the high-energy limit, which seems to be a suitable approximation for the conditions in discussion. The corresponding amplitude can be cast into the impact-factor representation [28]:

$$A(g_{\lambda_1} g_{\lambda_2} \rightarrow V_{\lambda_3} V_{\lambda_4}; s, t) = is \int d^2 \kappa \frac{\mathcal{J}(g_{\lambda_1} \rightarrow V_{\lambda_3}; \kappa, \mathbf{q}) \mathcal{J}(g_{\lambda_2} \rightarrow V_{\lambda_4}; -\kappa, -\mathbf{q})}{[(\kappa + \mathbf{q}/2)^2 + \mu_G^2][(\kappa - \mathbf{q}/2)^2 + \mu_G^2]}, \quad (1)$$

and the cross section reads

$$\frac{d\sigma(gg \rightarrow VV; s)}{dt} = \frac{\mathcal{N}_c}{64\pi s^2} \sum_{\lambda_i} \left| A(g_{\lambda_1} g_{\lambda_2} \rightarrow V_{\lambda_3} V_{\lambda_4}; s, t) \right|^2. \quad (2)$$

Here the subscripts λ_i denote the helicities of the gluons g and vector mesons V , and \mathbf{q} is the transverse momentum transfer, $t \approx -\mathbf{q}^2$. The overall color structure of the reaction is described by the factor $\mathcal{N}_c = (N_c^2 - 4)^2 / [16N_c^2(N_c^2 - 1)]$, where $N_c = 3$. We kept explicit an effective gluon mass μ_G which is responsible for soft QCD effects [30] and plays the role of regularization

parameter. However, in the present study we can safely set it to zero, and the amplitude remains finite as the impact factors \mathcal{J} vanish when $\boldsymbol{\kappa} \rightarrow \pm \mathbf{q}/2$. See also the discussion in [31].

At small t , within the diffraction cone, the cross section is dominated by the s -channel helicity conserving amplitude. In this case, the explicit form of the impact factor is

$$\mathcal{J}(g_\lambda \rightarrow V_\tau; \boldsymbol{\kappa}, \mathbf{q}) = \delta_{\lambda, \tau} \sqrt{4\pi\alpha_s^3} \int \frac{\psi(z, \mathbf{k}) I(z, \mathbf{k}, \mathbf{q})}{z(1-z)(2\pi)^3} dz d^2\mathbf{k}, \quad (3)$$

where $\psi(z, \mathbf{k})$ is the light-cone wave function of the vector meson and z is the light-cone momentum fraction carried by the heavy quark. Neglecting the intrinsic motion of the quarks we set $\psi(z, \mathbf{k}) = C \delta(z - \frac{1}{2}) \delta^{(2)}(\mathbf{k})$, where the normalizing constant C is adjusted to the J/ψ leptonic width and is related to the radial wave function at the origin as $C^2 = 12\pi^5/(N_c^2 m_\psi^3) |\mathcal{R}(0)|^2$. Within the above approximation, we have

$$I(z, \mathbf{k}, \mathbf{q}) = \frac{m_\psi}{2} \left[\frac{1}{\boldsymbol{\kappa}^2 + m_\psi^2/4} - \frac{4}{\mathbf{q}^2 + m_\psi^2} \right]. \quad (4)$$

Including the quark intrinsic motion would decrease the amplitude; for a more detailed analysis see [31]. As it will become clear from the numerical results, the non-relativistic approximation is sufficiently accurate for our purposes.

The cross section for the two-gluon exchange contribution to the $p + p \rightarrow J/\psi + J/\psi + X$ reaction (see Fig. 2) is calculated in the collinear approximation with MSTW2008(NLO) gluon distribution function [29] and the factorization scale $\mu_f^2 = m_t^2$, where m_t is the J/ψ transverse mass. The elementary $g+g \rightarrow J/\psi + J/\psi$ cross section can be easily calculated in the high-energy approximation similarly to how it was done for the $\gamma + \gamma \rightarrow J/\psi + J/\psi$ reaction [31]. The corresponding cross section is proportional to $\alpha_s^6(\mu_r^2)$, and therefore depends strongly on the choice of the renormalization scale. In the calculation presented here we take $\mu_r^2 = m_t^2$. In the high-energy approximation, the matrix element is merely a function of the transverse momentum \mathbf{q} of one of the J/ψ 's. This cannot be true at low subprocess energy, close to the J/ψ J/ψ threshold. Here one must take into account also the longitudinal momentum transfer. We therefore replace \mathbf{q}^2 by the exact \hat{t} or \hat{u} for the t and u diagrams respectively. We neglect here the possible interference between the box diagram and the two-gluon exchange mechanism, which is formally of lower order than the square of the two-gluon amplitude. However, firstly, the addition of box and two-gluon exchange amplitudes is not warranted without the consistent evaluation of α_s -corrections to the box. Secondly, it will become obvious from the numerical results, that the two-gluon mechanism is exceedingly small in the region of invariant masses dominated by the box mechanism.

B. DPS contributions

Under the hypothesis of having two independent hard partonic subprocesses A and B in a single pp collision, and under further assumption that the longitudinal and transverse components of generalized parton distributions factorize from each other, the inclusive DPS cross section reads (for details see, e.g., the recent review [1] with many references to prior works listed therein)

$$\sigma_{\text{DPS}}^{\text{AB}} = \frac{m}{2} \frac{\sigma_{\text{SPS}}^A \sigma_{\text{SPS}}^B}{\sigma_{\text{eff}}}, \quad (5)$$

$$\sigma_{\text{eff}} = \left[\int d^2b (T(\mathbf{b}))^2 \right]^{-1}, \quad (6)$$

where $T(\mathbf{b}) = \int f(\mathbf{b}_1) f(\mathbf{b}_1 - \mathbf{b}) d^2b_1$ is the overlap function that characterizes the transverse area occupied by the interacting partons, and $f(\mathbf{b})$ is supposed to be a universal function of the impact parameter \mathbf{b} for all kinds of partons with its normalization fixed as

$$\int f(\mathbf{b}_1) f(\mathbf{b}_1 - \mathbf{b}) d^2b_1 d^2b = \int T(\mathbf{b}) d^2b = 1. \quad (7)$$

The inclusive SPS cross sections σ_{SPS}^A and σ_{SPS}^B for the individual partonic subprocesses A and B can be calculated in a usual way using the single parton distribution functions. The symmetry factor m equals to 1 for identical subprocesses and 2 for the differing ones.

These simplifying factorization assumptions, though rather customary in the literature and quite convenient from the computational point of view, are not sufficiently justified and are currently under revision [1]. Nevertheless, we restrict ourselves to this simple form (5) regarding it as the first estimate for the DPS contribution. The presence of correlation term in the two-parton distributions results in reduction [32–34] of the effective cross section σ_{eff} with the growth of the hard scale, while the dependence of σ_{eff} on the total energy at a fixed scale is rather weak [33]. Thus, in fact, we obtain the lower bound estimate for the contribution under consideration. The CDF [35, 36] and D0 [37] measurements give $\sigma_{\text{eff}} \simeq 15$ mb, that constitutes roughly 20% of the total (elastic + inelastic) $p\bar{p}$ cross section at the Tevatron energy. We will use this value in our further analysis.

When calculating the inclusive SPS cross section $\sigma_{\text{SPS}}^{J/\psi}$ we take into account both the direct production channel $g+g \rightarrow J/\psi + g$ and the production of P -wave states $g+g \rightarrow \chi_{cJ}$ followed by radiative transitions $\chi_{cJ} \rightarrow J/\psi + \gamma$. Numerically these two production mechanisms turn to be of approximately equal importance. The calculation of the relevant Feynman diagrams is straightforward, but is done in the k_t -factorization approach implying that the initial gluon spin density matrix is taken in the form $\bar{\epsilon}_g^\mu \epsilon_g^{*\nu} = k_T^\mu k_T^\nu / |k_T|^2$ (similarly to what we did for the "box" SPS subprocess). The computational technique is explained in every detail in Ref. [18].

The formation probability of J/ψ meson is determined by its radial wave function; the latter is extracted from the known leptonic decay width [17] and is set to $|\mathcal{R}_\psi(0)|^2 = 0.8 \text{ GeV}^3$. The formation probability of χ_{cJ} mesons is determined by the derivative of the radial wave function; the latter is taken from the potential model [38]: $|\mathcal{R}'_\chi(0)|^2 = 0.075 \text{ GeV}^5$. The decay branchings are taken from the Particle Data Book [17]: $Br(\chi_{c1} \rightarrow J/\psi \gamma) = 35\%$, $Br(\chi_{c2} \rightarrow J/\psi \gamma) = 20\%$. The decay angular distributions are generated in accordance with the calculated χ_{cJ} polarization properties under the assumption of electric dipole dominance [39].

III. RESULTS AND DISCUSSION

We start with discussing the role of kinematic restrictions on the J/ψ transverse momentum. Shown in Fig. 3 are the fractions of SPS events surviving after imposing cuts on $p_T(\psi)$. Dashed line corresponds to requiring $p_T(\psi) > p_{T,min}$ for only one (arbitrarily chosen) J/ψ meson with no restrictions on the other. Were the two J/ψ 's produced independently, the probability of having $p_T(\psi) > p_{T,min}$ for the both J/ψ 's simultaneously could be obtained by just squaring the single-cut probability (dash-dotted curve in Fig. 3). On the contrary, in the naive the back-to-back kinematics, a cut applied to any of the two J/ψ 's would automatically mean the same restriction on the other, thus making no effect on the overall probability (dashed curve). The DPS production mode with cuts applied to both J/ψ mesons is represented by the dotted curve in Fig. 3. As one can see, this curve is rather close to that modeling the idealized independent SPS production.

The explicit calculation (solid curve) lies between the two idealistic extreme cases related to the fully independent (dash-dotted curve) and fully back-to-back correlated (dashed curve) production of J/ψ pairs. In the region $p_{T,min} < 4 \text{ GeV}$ the solid and dash-dotted curves almost coincide, thus showing that the two J/ψ 's are nearly independent. With stronger cuts on $p_T(\psi)$, the curves diverge showing that the production of J/ψ 's becomes correlated.

Another illustration of this property is given by the distributions in the azimuthal angle difference $d\sigma(\psi\psi)/d\Delta\varphi$ exhibited in Fig. 4. The distribution looks flat for the unrestricted phase space (the upper plot), but tends to concentrate around $\Delta\varphi \simeq \pi$ when the cuts on $p_T(\psi)$ become tighter (the middle and the lower plots in Fig. 4.) In principle, one could get rid of the SPS contribution by imposing cuts like $p_T(\psi) > 6 \text{ GeV}$, $\Delta\varphi < \pi/4$, but the DPS cross section would then fall from tens of nanobarns to few picobarns. We can conclude that the SPS and DPS modes are potentially distinguishable at sufficiently high $p_T(\psi)$, but the production rates fall dramatically, and so, the practical discrimination of the production mechanisms remains problematic.

Now we turn to rapidity correlations explained in

Figs. 5 and 6. In the case of independent production (the DPS mode), the distribution over Δy is rather flat (dash-dotted curve in Fig. 5), while in the case of SPS 'box' contribution (dotted curve in Fig. 5) it is concentrated around $\Delta y \simeq 0$ and does not extend beyond the interval $|\Delta y| < 2$. The shape of the double-differential cross section $d\sigma/dy(\psi_1)dy(\psi_2)$ corresponding to the Leading-Order SPS contribution is presented in Fig. 6. This contribution forms a long diagonal 'ridge' in the $y(\psi_1) - y(\psi_2)$ plane.

In Fig. 5 we also show pseudo-diffractive contributions from the one- and two-gluon exchange processes of Fig. 2. As it was expected, these processes lead to relatively large Δy and even show maxima at $\Delta y \simeq \pm 2$. This corresponds to a typical situation with one J/ψ moving forward and the other one moving backward, following the directions of the initial gluons. The minimum for the two-gluon exchange $g + g \rightarrow J/\psi + J/\psi$ subprocess is a consequence of the educated guess correction of the high-energy formula at low energies as discussed above.

At the same time, the absolute size of the one-gluon exchange cross section is found to be remarkably small. There are several reasons taking credit for this smallness. First, is the presence of two extra powers of α_s . Second, is just the large typical rapidity difference that makes the invariant mass of the final state relatively large: $M_{\psi\psi}(\Delta y=2)/M_{\psi\psi}(\Delta y=0) \simeq \cosh(\Delta y/2)$. In turn, larger masses mean larger values of the probed x , and, accordingly, lower values of the gluon densities.

The third and the most important reason lies in the color factors. The color amplitude of the first diagram in the first row of Fig. 1 reads $\text{tr}\{T^a T^c T^c T^b\} = [(N_c^2 - 1)/(4N_c)]\delta^{ab}$ (where T stand for the $SU(3)$ generators). After taking square and summing over the initial gluon colors a and b it gives $[\frac{2}{3}\delta^{ab}]^2 = 32/9$. Similarly, for the diagrams in the second row we have $[\text{tr}\{T^a T^c T^d\} f^{bcd}]^2 = [\frac{1}{4}f^{acd} f^{bcd}]^2 = [\frac{N_c}{4}\delta^{ab}]^2 = 9/2$ and $[\text{tr}\{T^c T^d\} f^{ace} f^{bde}]^2 = [\frac{1}{2}f^{ace} f^{bce}]^2 = [\frac{N_c}{2}\delta^{ab}]^2 = 9$.

For comparison, the color amplitude of the first diagram in Fig. 2 reads $\frac{1}{4}d^{ace} \cdot \frac{1}{4}d^{bde}$, and the terms containing $\frac{1}{4}f^{ace}$ or $\frac{1}{4}f^{bde}$ disappear because of cancellations between the different diagrams. This yields after squaring

$$[\frac{1}{4}d^{ace}\frac{1}{4}d^{bde}]^2 = \frac{(N_c^2-1)(N_c^2-4)^2}{256 N_c^2} = \frac{1}{256} \frac{200}{9} \simeq 0.1.$$

The color interference term is even smaller (and negative):

$$\frac{[d^{ace}d^{bde}][d^{ade}d^{bce}]}{256} = \frac{(N_c^2-1)(N_c^2-4)(N_c^2-12)}{512 N_c^2} = \frac{-20}{256 \cdot 3}.$$

Note that all the considered contributions are of the same order in N_c .

The same suppression factors apply to the two-gluon exchange as well, but there is yet another suppressing mechanism specific for the one-gluon exchange process. It comes from the fact that the amplitude vanishes when

any of the final state gluons becomes soft (this property makes the process infrared-safe, as we have mentioned already). Recall that by the same token the inclusive production rates of J/ψ and χ_c mesons become comparable to each other in spite of the hierarchy of the wave functions (S -wave compared to P -wave). As a consequence, although the two-gluon exchange $g+g \rightarrow J/\psi+J/\psi$ and one-gluon exchange $g+g \rightarrow J/\psi+J/\psi+g+g$ processes are of the same QCD order, their magnitudes are considerably different.

IV. CONCLUSIONS

We have considered the production of J/ψ pairs at the LHC energies via SPS and DPS processes taking into account several possible contributing subprocesses. We find it rather difficult to disentangle the SPS and DPS modes on the basis of azimuthal or transverse momentum correlations: the difference becomes only visible at sufficiently high p_T , where the production rates are, indeed, very small.

Selecting large rapidity difference events looks more promising. The leading order SPS contribution is localized inside the interval $|\Delta y| \leq 2$ (and continues to fall down steeply with increasing $|\Delta y|$), while the higher order contributions extending beyond these limits are heavily suppressed by the color algebra and do not constitute significant background for the DPS production.

Acknowledgments

The authors thank Ivan Belyaev for useful discussions on many experimental issues. This work is supported in part by the Polish Grants DEC-2011/01/B/ST2/04535 and N N202 236 640, by the Russian Foundation for Basic Research Grants No. 10-02-93118 and 11-02-01454, by the FASI State contract 02.740.11.0244, by the President of Russian Federation Grant No 3920.2012.2, by the Ministry of Education and Sciences of Russian Federation under agreement No. 8412, and by the DESY Directorate in the framework of Moscow-DESY project on Monte-Carlo implementations for HERA-LHC.

-
- [1] P. Bartalini *et al.* arXiv:1111.0469.
 - [2] R. Aaij *et al.* (LHCb Collaboration), Phys. Lett. B **707**, 52 (2012).
 - [3] A.V. Berezhnoy, A.K. Likhoded, A.V. Luchinsky, and A.A. Novoselov, Phys. Rev. D **84**, 094023 (2011).
 - [4] A.A. Novoselov, arXiv:1106.2184.
 - [5] C.-H. Kom, A. Kulesza, and W.J. Stirling, Phys. Rev. Lett. **107**, 082002 (2011).
 - [6] S.P. Baranov, A.M. Snigirev, and N.P. Zotov, Phys. Lett. B **705**, 116 (2011).
 - [7] S.P. Baranov, Phys. Rev. D **84**, 054012 (2011).
 - [8] C.-H. Kom, A. Kulesza, and W.J. Stirling, Eur. Phys. J. C **71**, 1802 (2011).
 - [9] M. Luszczak, R. Maciula and A. Szczurek, Phys. Rev. D **85** 094034 (2012).
 - [10] W. Schäfer and A. Szczurek, Phys. Rev. D **85** 094029 (2012).
 - [11] C.-H. Chang, Nucl. Phys. B **172**, 425 (1980).
 - [12] R. Baier and R. Rückl, Phys. Lett. B **102**, 364 (1981).
 - [13] E.L. Berger and D. Jones, Phys. Rev. D **23**, 1521 (1981).
 - [14] L.V. Gribov, E.M. Levin, and M.G. Ryskin, Phys. Rep. **100**, 1 (1983); E.M. Levin and M.G. Ryskin, Phys. Rep. **189**, 268 (1990).
 - [15] S. Catani, M. Ciafaloni, and F. Hautmann, Phys. Lett. B **242**, 97 (1990); Nucl. Phys. B **366**, 135 (1991).
 - [16] J.C. Collins and R.K. Ellis, Nucl. Phys. B **360**, 3 (1991).
 - [17] J. Beringer *et al.* (Particle Data Group), Phys. Rev. D **86**, 010001 (2012).
 - [18] S.P. Baranov, A.V. Lipatov, and N.P. Zotov, Phys. Rev. D **85**, 014034 (2012).
 - [19] J.A.M. Vermaseren, *Symbolic Manipulations with FORM* (Computer Algebra Nederland, Kruislaan, SJ Amsterdam, 1991, ISBN 90-74116-01-9).
 - [20] B. Humpert and P. Mèry, Z. Phys. C **20**, 83 (1983); Phys. Lett. B **124**, 265 (1983).
 - [21] R.E. Ecclestone and D.M. Scott, Z. Phys. C **19**, 29 (1983).
 - [22] S.P. Baranov and H. Jung, Z. Phys. C **66**, 647 (1995).
 - [23] C.-F. Qiao, L.-P. Sun, and P. Sun, J. Phys. G **37**, 075019 (2010).
 - [24] P. Ko, J. lee, and C. Yu, JHEP **1101**, 070 (2011).
 - [25] H. Jung *et al.*, Eur. Phys. J. C **70**, 1237 (2010).
 - [26] H. Jung, <http://www.desy.de/~jung/cascade/updf.html>; Mod. Phys. Lett. A **19**, 1 (2004).
 - [27] V.V. Kiselev, A.K. Likhoded, S.R. Slabospitsky, and A.V. Tkabladze, Yad. Fiz. **49**, 1681 (1989)[Sov. J. Nucl. Phys. **49**, 1041 (1989)].
 - [28] I.F. Ginzburg, S.L. Panfil, and V.G. Serbo, Nucl. Phys. B **296**, 569 (1988).
 - [29] A.D. Martin, W.J. Stirling, R.S. Thorne and G. Watt, Eur.Phys. J. C **63** 189 (2009).
 - [30] N.N. Nikolaev, B.G. Zakharov, and V.R. Zoller, JETP Lett. **59**, 6 (1994); JETP Lett. **66**, 138 (1997).
 - [31] S.P. Baranov, A. Cisek, M. Klusek-Gawenda, W. Schäfer, and A. Szczurek, arXiv:1208.5917.
 - [32] M.G. Ryskin and A.M. Snigirev, Phys. Rev. D **83**, 114047 ((2011).
 - [33] C. Flensburg, G. Gustafson, L. Lonnblad, and A. Ster, JHEP **06**, 066 (2011).
 - [34] A.M. Snigirev, Phys. Rev. D **81**, 065014 (2010).
 - [35] F. Abe *et al.* (CDF Collaboration), Phys. Rev. D **47**, 4857 (1993).
 - [36] F. Abe *et al.* (CDF Collaboration), Phys. Rev. D **56**, 3811 (1997).
 - [37] V.M. Abazov *et al.* (D0 Collaboration), Phys. Rev. D **81**, 052012 (2010).
 - [38] E. J. Eichten and C. Quigg, Phys. Rev. D **52**, 1726 (1995).
 - [39] P. Cho, M.B. Wise, and S.P. Trivedi, Phys. Rev. D **51**, R2039 (1995).

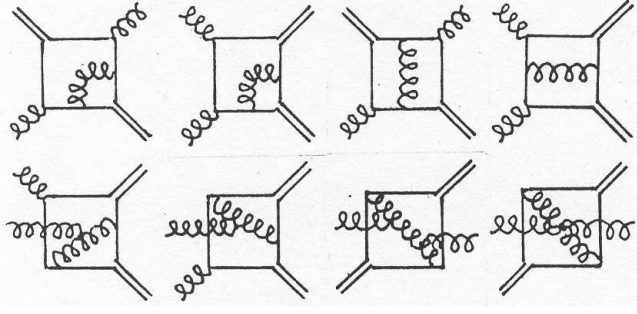


FIG. 1: Examples of Feynman diagrams representing the leading-order gluon-gluon fusion subprocess $gg \rightarrow J/\psi J/\psi$.

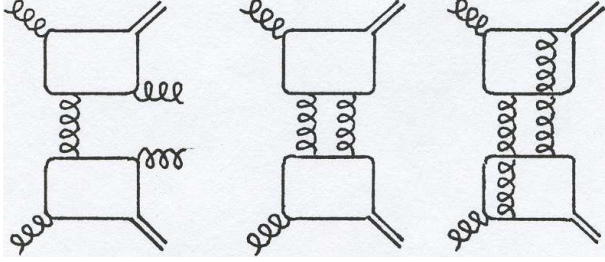


FIG. 2: Examples of Feynman diagrams representing the production of J/ψ pairs in pseudo-diffractive gluon-gluon scattering via one-gluon exchange and two-gluon exchange mechanisms.

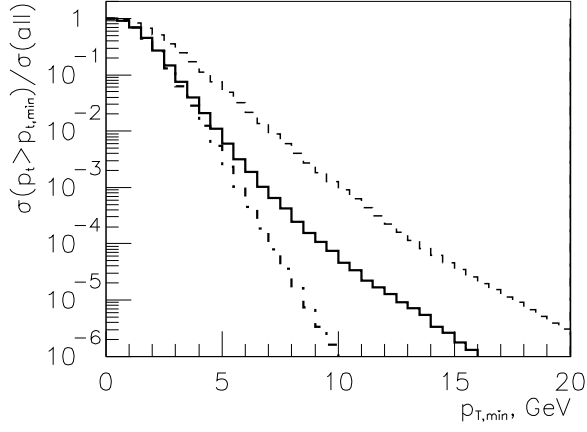


FIG. 3: Fraction of the production cross section left after imposing cuts on the J/ψ transverse momentum. Dashed curve, SPS mode under the requirement that one J/ψ meson has $p_T(\psi) > p_{T,min}$; dash-dotted curve, the square of the dashed curve; solid curve, SPS mode under the requirement that both J/ψ 's have $p_T(\psi) > p_{T,min}$; dotted curve, DPS mode under the requirement that both J/ψ 's have $p_T(\psi) > p_{T,min}$.

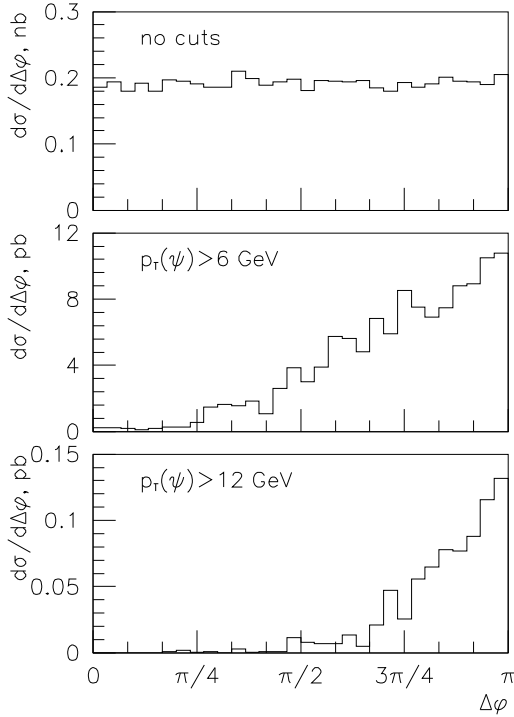


FIG. 4: Azimuthal angle difference distributions after imposing cuts on the J/ψ transverse momenta. Upper plot, no cuts; middle plot, $p_{T,min} = 6$ GeV; lower plot, $p_{T,min} = 12$ GeV.

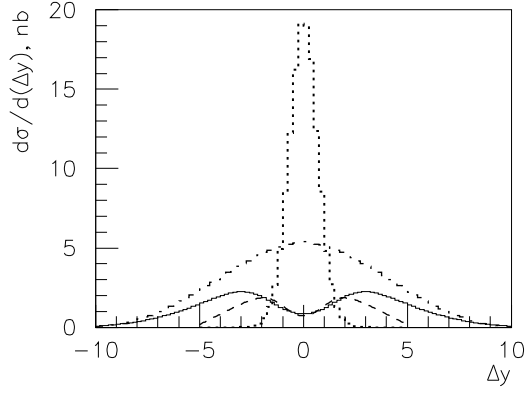


FIG. 5: Distribution over the rapidity difference between J/ψ mesons. Dotted curve, SPS 'box' contribution; dashed curve, one-gluon exchange contribution multiplied by 1000; solid curve, two-gluon exchange contribution multiplied by 25; dash-dotted curve, DPS production.

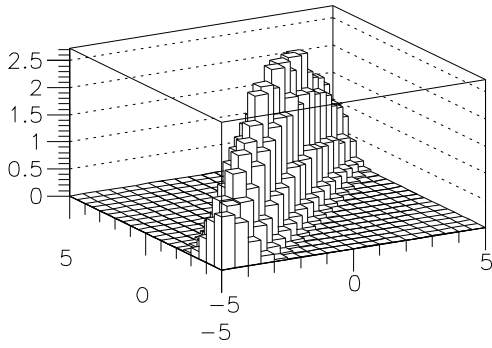


FIG. 6: Double differential distribution $d\sigma/dy(\psi_1)dy(\psi_2)$ for the Leading-Order SPS production mode.